Polarons in Ladder-Type Polymer Films; Recombination Channels and Electron−Phonon Coupling†

M. Wohlgenannt, C. P. An, and Z. V. Vardeny*

Department of Physics, University of Utah, Salt Lake City, Utah 84112

Received: September 21, 1999

We applied the photomodulation spectroscopy for probe-photon energies from 0.05 to 2.5 eV in films of ladder-type poly(*p*-phenylene) and identified a photoinduced absorption (PA) band related to triplet excitons and two correlated PA bands due to charged polarons. The low energy polaron band peaks at a relatively low photon energy of ∼0.1 eV, showing small polaronic relaxation energy. We employed photoinduced absorption-detected magnetic resonance spectroscopy to study the polaron recombination channels and found that spin $^1/_2$ magnetic resonance enhances the bimolecular recombination of polarons to singlet byproducts (singlet excitons and bipolarons). However, it reduces polaron recombination to triplet byproducts, such as triplet excitons. The low-energy polaron PA shows antiresonances due to its overlap with Raman- and IR-active vibrations. The antiresonances spectrum is compared to the IR and Raman spectra and found to also contain modes that are silent in the latter spectra.

I. Introduction

Polarons are the primary charged excitations in π-conjugated polymers (PCP) with nondegenerate ground states.[1] They are extended over several monomers and generate substantial lattice relaxation, which results in two energy levels inside the optical gap (Figure 1).[2] Polarons are also mobile, with an effective mass of order of the free-electron mass.[3] As a consequence of the two polaronic subgap levels, two below-gap optical transitions appear in the absorption spectra of charged PCP chains.[4] The physics of polarons is crucial to the understanding of charge transport in PCP films. In organic light emitting diodes (OLED), charge carriers are injected from electrodes into the active layer of PCP. The current is then passed through the polymer film in the form of polarons, which may recombine with oppositely charged polarons coming from the counter electrode to form singlet or triplet byproducts. For the spin component, there are three triplet sublevels, only one exists for singlets. Because only singlet states are luminescent, this puts a spin-statistical upper limit to the OLED quantum efficiency of 25%. However, OLEDs have been demonstrated to have quantum efficiencies as high as 50%,[5] which means that the formation cross-section for the singlet state must at least be three times larger than that found for triplet byproducts. It has been confirmed recently, by quantum chemical calculations,[6] that the singlet formation cross section generally exceeds the triplet cross section. Studying the polaron recombination channels may give important insight into the physics of OLEDs.

The continuous wave (cw) photomodulation (PM) spectroscopy has been widely used in PCP films and solutions to study the dynamics of long-lived photoexcitations with photoinduced absorption (PA) bands below the gap.[7−10] Photogenerated polarons have been studied using PM, by means of the two absorption bands inside the optical gap (Figure 1). Here, we have applied the PM technique in films of mLPPP (Figure 2, inset) down to probe photon energies of 0.05 eV. We found that the low energy polaron band peaks at a relatively low photon energy of ∼0.1 eV, demonstrating small polaronic relaxation[1] in mLPPP that is consistent with the polymer's rigid backbone structure (Figure 2, inset).

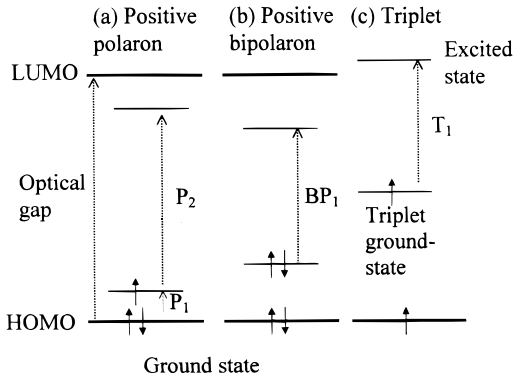

Figure 1. Schematic level diagram and optical transitions of (a) positive polaron, (b) positive bipolaron, and (c) triplet exciton.

Photogenerated polarons in films may recombine the same way as they do in OLEDs to singlet and triplet byproducts. We employed photoinduced absorption detected magnetic resonance (PADMR) spectroscopy to study the recombination channels of polarons to singlet and triplet states. PADMR leads to resonant changes in the recombination rates. We show that PADMR spin $^1/_2$ resonance increases polaron recombination to singlet states and decreases recombination to triplet states.

The charged polarons also cause the appearance of infrared active vibrations.[3,11] The low-energy polaronic PA overlaps with the spectral range of vibrational transitions (both IR and Raman active). We show that this leads to the creation of antiresonances,[12−14] in the PM spectrum arising from IR, Raman, and silent modes.

II. Experimental Section

PM spectroscopy has been widely used in PCP for studying long-lived photoexcitations with associated PA bands.[7−10] Two light beams are used in PM spectroscopy. For the excitation

† Part of the special issue "Harvey Scher Festschrift".

10.1021/jp993370m CCC: $19.00
Published on Web 03/24/2000

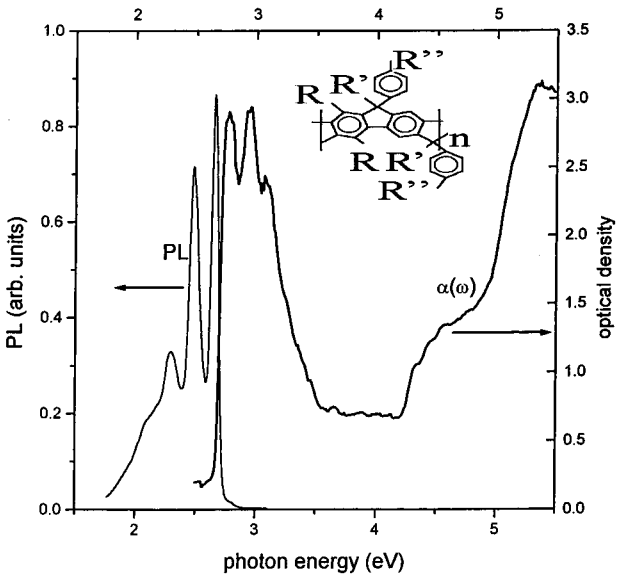

Figure 2. Photoluminescence (PL, solid) and absorption ($\alpha(\omega)$, bold) spectra of a mLPPP film. The inset shows the mLPPP repeat unit.

beam, we used an Ar^+ laser, the intensity of which was modulated with a chopper. A combination of various incandescent lamps (xenon, tungsten−halogen, and glowbar), diffraction gratings, optical filters, and solid-state detectors (silicon, germanium, indium antimonide, and mercury cadmium teluride) was used to span the probe photon energy, $\hbar\omega$, between 0.15 and 3 eV. The PM spectrum (vs $\hbar\omega$) was obtained by dividing the pump beam induced changes in the probe beam transmission, $\Delta T(\omega)$, by the probe beam transmission, $T(\omega)$, where ΔT was measured by a phase-sensitive technique; in this case, the PA, or $\Delta\alpha$ ($= -d^{-1}\Delta T/T$, where d is the film thickness) does not depend on the system's photon energy response.

We extended the probe photon $\hbar\omega$ down to 0.05 eV using a Fourier Transform Infrared (FTIR) spectrometer in combination with a deuterated triglycine sulfide (DTGS) detector. To obtain the PA spectrum, we measured the FTIR absorption spectrum with the pump beam on and, subsequently, with the pump beam blocked. We calculated the difference in transmission and repeated this alternation about 10 000 times to achieve a signal-to-noise ratio on the order of 10^{-5} in PA. Finally, the results were normalized by the sample transmission.

The spin associated with the PA bands may be obtained by PADMR.[15,16] In PADMR, we measure the changes in PA induced by a modulated μ-wave field (in our experiment, at 3 GHz) in resonance with the Zeeman split spin $^1/_2$ sublevels in magnetic field H.[15,16] The μ-wave resonant absorption leads to small changes, δT, in T. This δT is proportional to δN induced by the μ-waves, caused by changes in the recombination rates. Two types of PADMR spectra are possible:[16] The H-PADMR spectrum, in which δT is measured at a fixed probe wavelength λ as the magnetic field H is scanned, and the λ -PADMR spectrum, in which δT is measured at a constant H, in resonance, whereas λ is scanned.

The IR absorption spectra were measured with the FTIR spectrometer, whereas the Raman spectra were taken with nonresonant excitation (TiSapphire line) using a double monochromator and a photomultiplier tube (photon counter). For a review on Raman scattering from PCP, see reference 17 and references therein.

The measurements in this paper were done on an mLPPP film that was drop cast from a toluene solution with a concentration of ~5 mg/mL.

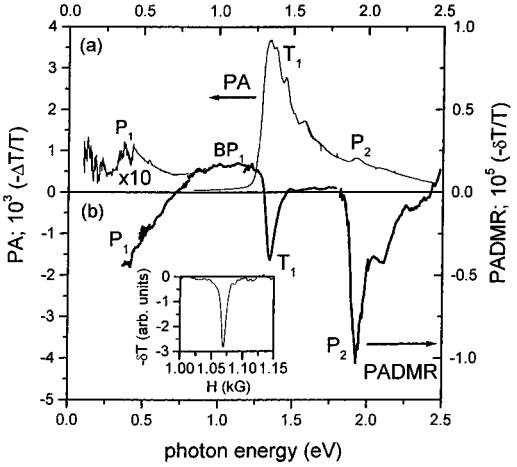

Figure 3. PA spectrum of an mLPPP film, excited at 3.5 eV and measured at 80 K, compared to the spin $^1/_2$ λ-PADMR spectrum, excited at 2.7 eV measured at $H = 1065$ G ($g = 2$) and 10 K. The inset shows the H-PADMR spectrum of spin $^1/_2$ at 1.9 eV.

III. Results and Discussion

In Figure 2, we show the polymer repeat unit (inset), the optical absorption, $\alpha(\omega)$, and the photoluminescence, PL, spectra of the mLPPP film used in our measurements. At low photon energies, $\alpha(\omega)$ consists of a three-peaked structure at 2.75, 2.93, and 3.11 eV, respectively, which we interpret as an optical transition into the lowest odd-parity exciton ($1B_u$) (0−0 transition) and its two phonon replica, 0−1 and 0−2, approximately 180 meV apart. At high photon energies, $\alpha(\omega)$ also contains absorption bands at 4.5 and 5.3 eV, respectively, which are interpreted as being due to transitions into higher but more localized excitons.[18] The PL spectrum is much sharper than $\alpha(\omega)$, but it too contains a pronounced three-peak feature, which is Stokes-shifted from that in $\alpha(\omega)$ by ~0.1 eV. Using an integrating sphere, we measured the absolute PL quantum efficiency in mLPPP to be about 30%.

PM SPECTRUM. In Figure 3a, we show the PM spectrum of the mLPPP film at temperature $\theta = 80$ K, excited at $E = 3.5$ eV in the spectral range from 0.15 to 2.5 eV. The PM spectrum is dominated by the PA band T_1 at 1.3 eV and also by the two correlated PA bands: P_1 below 0.7 eV and P_2 at 1.9 eV. A series of sharp photoinduced IR-active vibrations (IRAVs), which are correlated by their f and θ dependencies with the PA bands P_1 and P_2, but not with T_1, are also seen at $\hbar\omega < 0.25$ eV.[19,20] The photoinduced IRAVs indicate that charge carriers are photogenerated in the polymer chains. Therefore, their correlation with P_1 and P_2, but not with T_1, shows that the former bands are due to long-lived *charged* excitations, whereas the latter band is caused by long-lived *neutral* excitations.

We now turn our attention to the P_1 band (see Figure 3a), which is the low-energy polaronic transition. The use of a Fourier Transform Infrared (FTIR) spectrometer allows us to complete the PA spectrum down to $\hbar\omega = 0.05$ eV. The obtained FTIR PA spectrum is shown in Figure 4. What appeared to be IRAV peaks in Figure 3, now reveal themselves to be anti-resonances (AR)[12,13] peaking downward from the P_1 PA band, whose shape is indicated by the dotted line in Figure 4. This also explains why parts of the spectrum stretch below zero. It is shown below that a reasonable agreement between the photoinduced modes and Raman and IR active modes of mLPPP may be achieved only if the AR are compared. The P_1 band

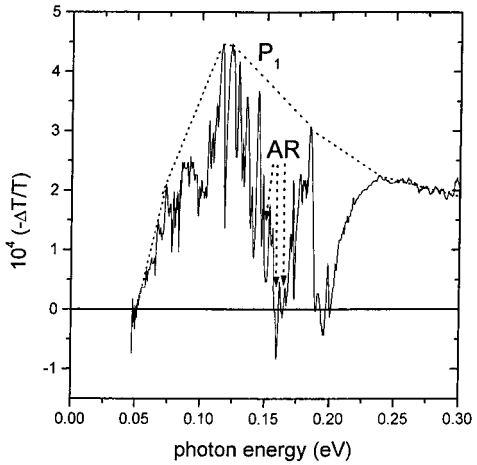

Figure 4. PA spectrum excited at 3.5 eV and measured at 80 K in the probe photon energy range of 0.05 to 0.3 eV as obtained with a FTIR spectrometer. The dotted line illustrates the spectral shape of the P_1 band as a guide to the eye, whereas the IRAVs appear as antiresonances (AR).

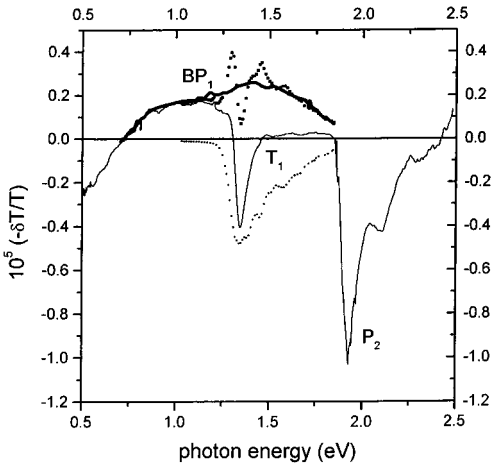

Figure 5. Spin $^1/_2$ λ-PADMR spectrum as measured (solid line) after subtracting (dotted, bold) the triplet PA band T_1 (dotted) and crude smoothing (bold) to obtain the PADMR bipolaron band (BP_1).

peaks at a relatively low $\hbar\omega$, ~0.1 eV, demonstrating small chain relaxation for polarons in mLPPP, in agreement with the polymer's rigid backbone structure.

PADMR SPECTROSCOPY. The H-PADMR spectrum of mLPPP at $\hbar\omega = 1.9$ eV is shown in the inset of Figure 3b. We observed a negative resonance in PA (i.e., $\delta T > 0$) at 1065 G because of the enhanced recombination of spin $^1/_2$ photoexcitations. The λ-PADMR spectrum, measured at $H = 1065$ G, is shown in Figure 3b and compared to the PA spectrum. The λ-PADMR spectrum contains a sharp band at 1.9 eV, which coincides in energy with the P_2 band. This is followed by two phonon replica at 2.1 and 2.3 eV, respectively. We note the remarkable ability of PADMR to elucidate small PA bands, such as P_2, which are covered by much stronger bands, such as T_1 in the PM spectrum (Figure 3a). The corresponding λ-PADMR of the P_1 band appears at $\hbar\omega$ below 0.7 eV. The λ-PADMR spectrum also shows that T_1 is much less correlated with spin $^1/_2$ excitations. In fact, we also note that P_1 and P_2 bands coincide in energy with the two doping-induced absorption bands in mLPPP caused by polarons,[19] and that T_1 is close in energy to the long-lived excitations in isolated PPP oligomers assigned to triplets (see Figure 1).[20] On the basis of these facts and the spectroscopies described above, we conclude that P_1 and P_2 PA bands are due to photogenerated *polarons*, whereas T_1 is caused by photoexcited *triplet excitons*.

We now turn our attention to a region in the PADMR spectrum of resonance-enhanced absorption, namely, $\delta\alpha > 0$ between about 0.8 and 1.3 eV; at higher energies than 1.2 eV, it overlaps with the sharper spin $^1/_2$ resonance of the triplet exciton. To get a better idea of its spectral shape, we subtracted the triplet PA band from the PADMR spectrum. We obtain (Figure 5) a broad band centered around ~1.3 eV. In polyfluorene, a PCP with a PM spectrum very similar to that of mLPPP, a similar positive PADMR band has been observed[21] in the same spectral region, although it is stronger and with a pronounced peak shape. A relatively broad band centered at 1.4 eV was also found in charge-induced absorption spectroscopy of mLPPP devices at high driving currents.[22] A single positive λ-PADMR band between the two polaron bands, P_1 and P_2, is commonly interpreted[4] as being due to bipolarons (BP). Bipolarons[1,23] are the doubly charged carriers in PCP and are predicted to be energetically favored when compared to a

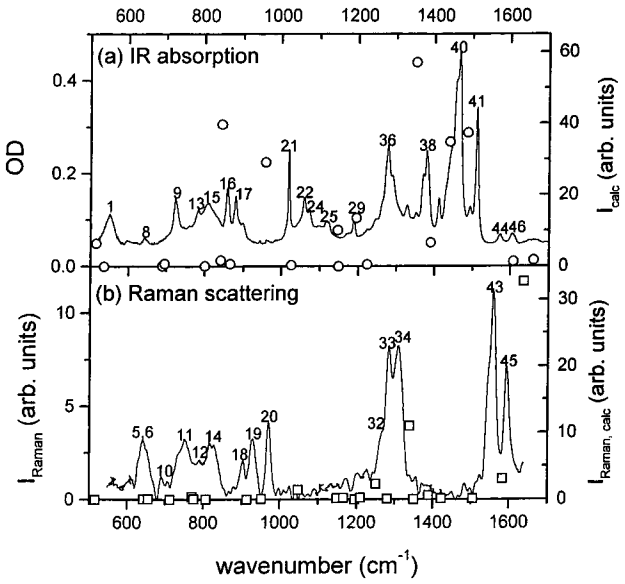

Figure 6. IR (a) and Raman (b) spectra of a mLPPP film. The solid lines are experimental curves; the circles and squares give calculated intensities and frequencies for IR (a) and Raman (b), after reference 24. The experimental IR- and Raman-modes have been assigned numbers in reference to Table 1.

pair of separate, equally charged polarons. They are characterized by a single subgap absorption band (Figure 1) and are spinless.

All three of the spin $^1/_2$ PADMR resonances, that of polaron, bipolaron, and triplet, and their respective signs, may be understood through a recombination model: In general, polarons may recombine in the following channels:

(i) Two spin antiparallel polarons of opposite charge may recombine to form a singlet exciton, which will then decay to the groundstate ($P^+ \uparrow + P^- \downarrow \rightarrow$ SE $\rightarrow$ GS). (ii) Two spin antiparallel polarons of equal charge may "recombine" to form a bipolaron ($P^+ \uparrow + P^+ \downarrow \rightarrow$ BP). (iii) Two spin parallel polarons of opposite charge may "recombine" to form a triplet exciton ($P^+ \uparrow + P^- \uparrow \rightarrow$ TE).

Because the resonant microwave absorption equalizes the population of both Zeeman levels, it increases the probability for polarons to find opposite spin partners to form singlet byproducts and, by the same amount, reduces the probability of finding same spin partners to form triplet byproducts. This explains the increase in bipolarons, a singlet excitation, and the

TABLE 1. Summary of Experimental IR, Photoinduced (IRAV), Antiresonances (AR), and Raman Vibrational Modes and Assignment to Calculated Frequencies after Reference 24.[a]

vibration	IR (cm^{-1})	AR (cm^{-1})	Raman (cm^{-1})	calculated (cm^{-1})
1	550			515
2		525		515
3		560		536
4		605		
5		625	640	642
6		644	640	655
7		665		
8	640			689
9	725	730		695
10			695	712
11		745	750	770
12			790	775
13	785	785		801
14		830	820	807
15	810	805		844
16	855	860		841
17	880	880		866
18		905	900	
19			930	913
20		955	970	951
21	1020	1020		958
22	1060	1055		1026
23				1047
24	1070	1070		
25	1115	1115		1146
26		1135		1148
27				1149
28				1165
29	1190			1195
30		1210		1210
31		1245		1224
32			1265	1250
33		1270	1280	1280
34		1315	1305	1338
35		1340		1349
36	1275	1280		1351
37		1390		1388
38	1375	1375		1390
39				1422
40	1465	1460		1440
41	1510	1520		1487
42				1504
43		1565	1555	1582
44	1570			1608
45		1610	1590	1636
46	1605			1660

[a] The modes are numbered in the order of increasing frequency of the assigned calculated Mode.

reduction of triplets. The negative polaronic PADMR bands mean a net increase of polaron recombination, which shows that the increase in recombination to singlets outweighs the decrease of recombination to triplets.

IR AND RAMAN SPECTRA. Figure 6a,b show the IR and Raman spectra of the mLPPP film. In the case of the Raman spectrum, a background from elastically scattered light has been subtracted. The open circles in Figure 6a give the calculated IR spectrum from reference 24. Each IR mode is represented by an open circle, whose *x* component in the graph gives the mode's frequency, whereas the *y* component gives the calculated intensity. The same representation is chosen for the calculated Raman intensities (open squares in Figure 6b). In Figure 6, the experimental peaks have been assigned a number in reference to Table 1. Figure 7 shows the comparison between IR (a), PA antiresonances (b), and Raman (c) spectra in the spectral region from 500 to 1700 cm^{-1}. The IRAV antiresonances of the PM

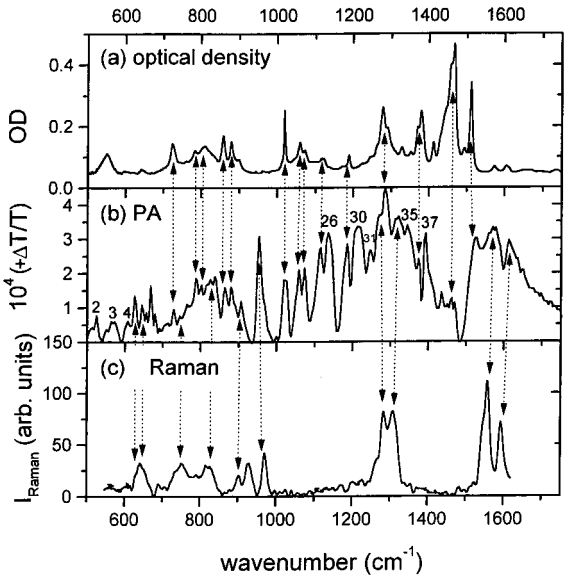

Figure 7. Comparison between IR absorption (a), photoinduced IRAVs (b), and Raman (c) spectra of mLPPP. The IRAV antiresonances have been converted to peaks by subtracting the dotted line of Figure 4 and inverting their sign. The arrows show the assignment of photoinduced IRAVs to IR- or Raman-active modes. Photoinduced IRAVs that cannot be assigned to experimental IR- or Raman-modes have been assigned a number in reference to Table 1.

spectrum have been converted to peaks by subtracting the dotted line of Figure 4 and inverting their sign. In Figure 7, the IRAVs with negative PA spectra have been assigned to peaks in the IR or Raman spectrum. The IRAVs that do not correspond to any IR or Raman peaks in Figure 6 have been assigned a number in reference to Table 1. We have, therefore, assigned a number to each IR or Raman mode and also to silent modes that appear only in the PA spectrum. Table 1 summarizes the IR-, photoinduced AR IRAV-, and Raman-mode frequencies and assigns them to the calculated mode frequency. We also found (see Table 1) vibrational modes that are silent in IR and Raman spectra (vibrations number 2, 3, 4, 26, 30, 31, 35, and 37), which appear as strong lines in the PA spectrum. We conclude that the PA technique with AR appearance may serve as a powerful tool to study the molecular vibration spectrum in PCP because it also contains silent modes.

IV. Conclusions

We have presented the PM spectrum of a mLPPP film at photon energies between 0.05 and 2.5 eV, as well as the PADMR spin $^1/_2$ spectrum. The PM spectrum is dominated by a triplet−triplet absorption at 1.3 eV and by two polaron absorption bands peaking at ~0.1 and 1.9 eV, respectively. We showed that the band at 1.9 eV has a strong spin $^1/_2$ resonance, whereas the PA band at 1.3 eV has a weaker spin $^1/_2$ resonance. We analyzed the spin $^1/_2$ PADMR spectrum and concluded that the spin $^1/_2$ resonance increases polaron "recombination" to singlet species, namely singlet excitons and bipolarons, and reduces recombination to triplets. The low energy polaron transition spectrally overlaps with IR and Raman transitions and exhibits antiresonances. These antiresonances arise from IR- and Raman-active modes and also from silent modes. Therefore, the PA technique with AR appearance may serve as a powerful tool to study the molecular vibration spectrum.

Acknowledgment. We thank U. Scherf and K. Muellen for the mLPPP powder and R. Österbacka for useful discussions.

The work was supported in part by the DOE, Grant No. FG-03-96 ER 45490, and the NSF, Grant No. DMR-9732820.

References and Notes

(1) Heeger, A. J.; Kievelson, S.; Schrieffer, J. R.; Su, W. P. *Rev. Mod. Phys.* **1988**, *60*, 781, and references therein.

(2) Fesser, K.; Bishop, A. R.; Campbell, D. K. *Phys. Rev. B* **1983**, *27*, 4804.

(3) Ehrenfreund, E.; Vardeny, Z. V.; Brafman, O.; Horowitz, B. *Phys. Rev. B* **1987**, *36*, 1535.

(4) Lane, P. A.; Wei, X.; Vardeny, Z. V. *Phys. Rev. Lett.* **1996**, *77*, 1544.

(5) Cao, Y.; Parker, I. D.; Yu, C.; Zhang, C.; Heeger, A. J. *Nature* **1999**, *397*, 414.

(6) Shuai, Z.; Beljonne, D.; Silbey, R. J.; Bredas, J. L. *Phys. Rev. Lett.* **2000**, *84*, 131.

(7) Saraciftci, N. S.; Smilowitz, L.; Heeger, A. J.; Wudl, F. *Science* **1992**, *258*, 1474.

(8) Graupner, W.; Leditzky, G.; Leising, G.; Scherf, U. *Phys. Rev. B* **1996**, *54*, 7610.

(9) Wei, X.; Vardeny, Z. V.; Saraciftci, N. S.; Heeger, A. J. *Phys. Rev. B* **1996**, *53*, 2187.

(10) Vardeny, Z. V.; Wei, X. *Handbook of Conducting Polymers II*; Marcel Dekker: New York, 1997; Chapter 22.

(11) Horowitz, B. *Solid State Commun.* **1982**, *41*, 729.

(12) Rice, M. J. *Phys. Rev. Lett.* **1976**, *37*, 36.

(13) Pratt, F. L.; Wong, K. S.; Hayes, W.; Bloor, B. *J. Phys. D* **1987**, *20*, 1361.

(14) Österbacka, R.; An, C. P.; Jiang, X. M.; Vardeny, Z. V. *Science* (in print).

(15) Wei, X.; Hess, B. C.; Vardeny, Z. V.; Wudl, F. *Phys. Rev. Lett.* **1992**, *68*, 666.

(16) Lane, P. A.; Wei, X.; Vardeny, Z. V. *Phys. Rev. B* **1997**, *56*, 4626.

(17) Gussoni, M.; Castiglioni, C.; Zerbi, G. *Spectroscopy of Advanced Materials*; John Wiley & Sons: New York, 1991; p 251.

(18) Chandross, M.; Mazumdar, S.; Liess, M.; Lane, P. A.; Vardeny, Z. V.; Hamaguchi, M.; Yoshino, K. *Phys. Rev. B* **1994**, *50*, 14 702.

(19) Graupner, W.; Mauri, M.; Stampfl, J.; Leising, G.; Scherf, U.; Müllen, K. *Solid State Commun.* **1994**, *91*, 7.

(20) Graupner, W.; Eder, S.; Mauri, M.; Leising, G.; Scherf, U. *Synth. Met.* **1995**, *69*, 419.

(21) Cadby A. J.; et al., *Proc. ICEL #2*; Sheffield, U.K. 5/1999 (*Synth. Met.*, in press).

(22) Wohlgenannt, M.; List, E. J. W.; Zenz, C.; Leising, G.; Graupner, W.; Vardeny, Z. V., to be published.

(23) Greenham, N. C.; Shinar, J.; Partee, J.; Lane, P. A.; Amir, O.; Lu, F.; Friend, R. H. *Phys. Rev. B* **1996**, *53*, 13 528.

(24) Cuff, L.; Kertesz, M. *J. Phys. Chem.* **1994**, *98*, 12 223